

UAL/ETEAPOT Proton EDM Benchmark Report IV: Comparison of ETEAPOT, Linearized Transfer Matrix, and Runge-Kutta Proton EDM Lattice Results (DRAFT)

R.M.. Talman and J.D. Talman

January, 2013

Abstract

Valeri Lebedev's new, all-electric proton EDM lattice, (here referred to as `E_ValLeb2-s14-RF.sxf`), which is strong-focusing radially, weak-focusing vertically, is treated as the most up-to-date lattice for purposes of benchmark comparison of various lattice calculation codes. For transverse optics the agreement among three independent analyses, two based on the Wollnik transfer matrix formalism, one using the ETEAPOT lattice simulation code, is excellent. Plots and tables bear this out. The understanding of longitudinal dynamics, though still murky, is clearer than previously. A crude comparison between ETEAPOT and Runge-Kutta analysis of longitudinal dynamics in a previous benchmark lattice `E_BM_Z-RF.sxf` is given. Factors making such comparisons delicate are discussed. The importance of proving beam capture into stable longitudinal buckets is emphasized. In fact, unlike `E_BM_Z-RF.sxf`, attempts to achieve stable capture into the `E_ValLeb2-s14-RF.sxf` lattice have failed so far. It is not known at present whether this is a property of the lattice, which would be surprising, or a bug in ETEAPOT.

1 Parameters of Benchmark Proton EDM Lattices

This section concentrates on treating the proton EDM lattice proposed by Valeri Lebedev[1] as the most up-to-date “benchmark comparison lattice”, following previous benchmark comparisons[2][3][4][5]. This lattice (in *standard exchange format* form it is `ValLeb2-s14.sxf`) has strong horizontal focusing and weak vertical focusing.

Transverse Twiss parameters have been calculated from linearized transfer matrices in two different ways, one described in this report, and referred to as R.M.T., and one from the initial Lebedev report[1] and referred to as V.L. Both of these analyses are based on the Wollnik[6] linearized transfer matrix formalism. As such, they are independent only as regards lattice details, element slicing, and interpretation of the formalism. The third analysis, based on ETEAPOT is here referred to as J.D.T. The ETEAPOT approach is to perform exact tracking in an approximate lattice, and to reconstruct the Twiss parameters by numerical post-processing the results from tracking a standard bunch of 21 small amplitude particles. Being based on entirely different formalisms, the comparison of ETEAPOT and Wollnik-based results can provide a stringent test of our understanding of the proposed proton EDM lattice.

Comparisons of transverse lattice parameters are given in Table 1. The R.M.T and J.D.T. analyses are based on lattice file `ValLeb2-s14.sxf` which has been reconstructed from the original Lebedev[1] report. The lattice is simple enough, and the Lebedev report careful and thorough enough, that this reconstruction could be performed with little ambiguity. The only significant uncertainty was that only the ratio of quadrupole fields GDD/GFF, rather than the absolute quad strengths (i.e. inverse focal lengths) is given in the report [1]. The tunes Q_x and Q_y are given, however, and, from these, the absolute (half-)quad strengths qFh and qDh have been determined.

Table 1: Transverse lattice parameters of the proton EDM lattice proposed by Valeri Lebedev[2], as evaluated in three independent ways. This lattice (here referred to as `ValLeb2-s14.sxf`) can serve as a new (most realistic so far) benchmark lattice.

Analysis method	author	half-quad strength qFh	quad ratio GDD/GFF or qDh/qFh	horz. tune Q_x	vert. tune Q_y	max. horz. β_x	min. horz. β_x	max. vert. β_y	min. vert. β_y
		1/m				m	m	m	m
linear tr.mat.	V.L.	-0.0307	-0.802	2.32	0.31	29.1	≈ 16	204	≈ 118
linear tr.mat.	R.M.T.	-0.0307	-0.765	2.32	0.315	29.2	15.4	201.8	114.0
ETEAPOT	J.D.T.	-0.0307	-0.765	2.31	0.325	29.2	15.4	196	110.8

In the `ValLeb2-s14.sxf` lattice description file, the “-s14” indicates that the bend elements have been artificially sliced by a factor of four, from about 9 meters to about 2.25 meters. This has been done both for making the physical construction more realistic, and to relieve the burden on ETEAPOT tracking over such long elements. As it happens, ETEAPOT automatically performs a further splitting of a factor of two, to make lattice parameters available at element centers. Also ETEAPOT can perform further splitting in order to represent bend elements having field indices other than $m = 0$ (which corresponds to “cylindrical” bent-planar, parallel electrodes). However for the present study we fix $m = 0$.

Table 1 shows excellent agreement among the three approaches. With qFh constrained to be identical for all studies, the only discrepancy is in the ratio qFh/qDh which differs at most by 4.6%, from -0.802 to -0.765. A discrepancy at least this large can be expected from the fundamental ambiguity in the treatment of electric elements, especially in the comparison between ETEAPOT and Wollnik approaches. As it happens there is essentially no difference in the treatments based on the identical lattice description file, and the entire discrepancy is between V.L. and R.M.T. implementations of the Wollnik approach on slightly different lattices. In any case all comparisons are sufficiently excellent that there can be no doubt the the transverse lattice performance will be essentially just as Lebedev has first stated. One must keep in mind, however, that the lattice with unbalanced focusing is quite “highly strung”. For example, a 1% change in the qDh focal length reduces Q_y from 0.3 to 0.0 (where the lattice becomes unstable).

R.M.T. linear transfer matrix Twiss functions are compared to J.D.T. ETEAPOT Twiss functions in Figures 1 and 2. V.L. linear transfer matrix Twiss functions are compared to ETEAPOT Twiss functions in Figures 3 and 4. There is essentially perfect agreement in all cases.

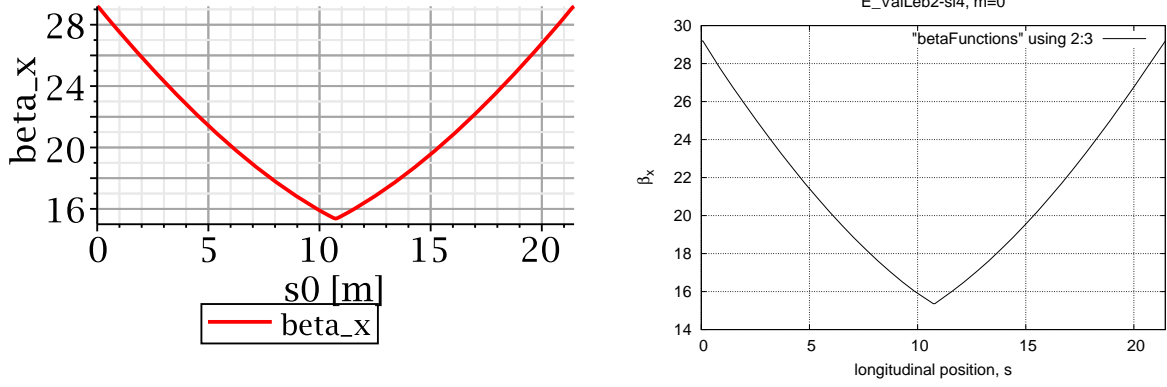


Figure 1: Proton EDM Lattice β_x functions as determined by linear transfer matrix formalism, on the left, and by ETEAPOT, on the right.

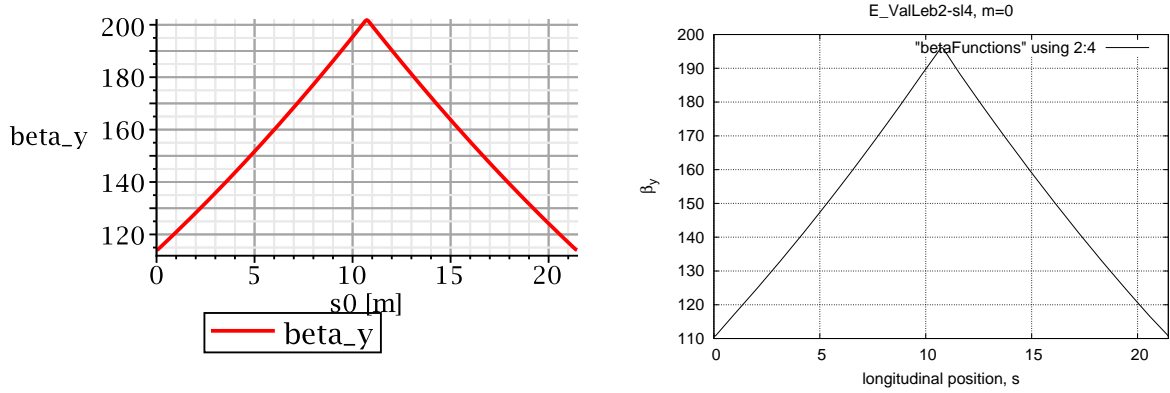


Figure 2: Proton EDM Lattice β_y functions as determined by linear transfer matrix formalism, on the left, and by ETEAPOT, on the right.

Figure 3, copied directly from the original Lebedev report, gives his beta functions and dispersions. For comparison the ETEAPOT plots are repeated in Figure 4. Again the agreement is excellent.

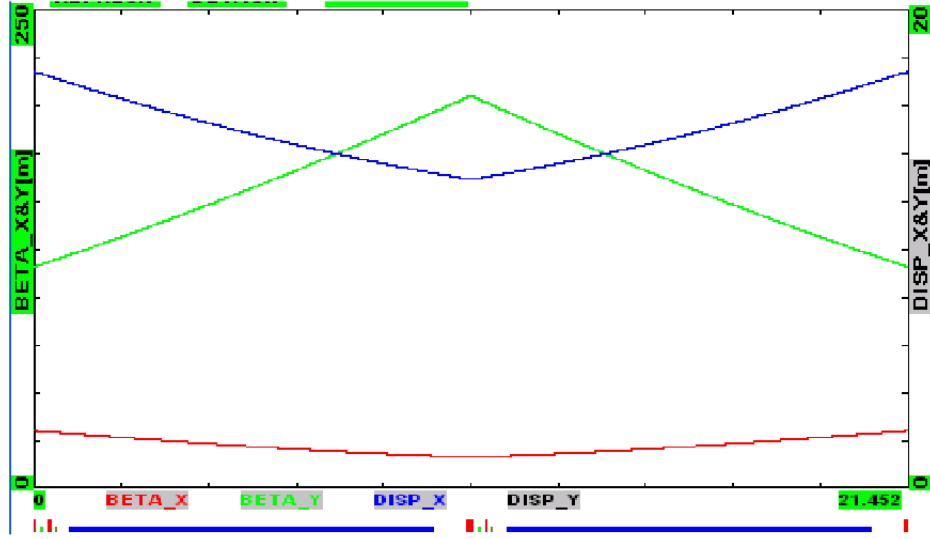


Figure 3: Proton EDM Lattice β functions as determined by Valeri Lebedev[1]. Also shown is the dispersion function.

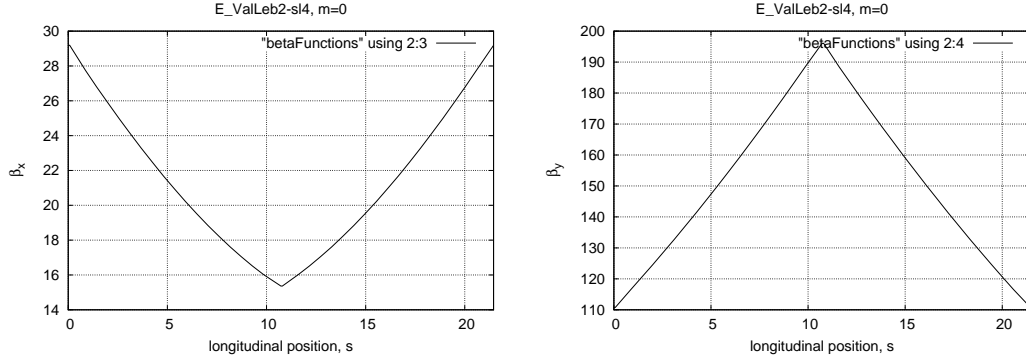


Figure 4: Proton EDM Lattice β functions as determined by ETEAPOT. Ambiguity in the definition of “dispersion” complicates comparison with the Lebedev dispersion. Though not yet completed, there is every reason to expect similarly good agreement.

2 Comparison of Longitudinal Dynamics

Though transverse dynamics in all-electric proton EDM rings is now completely under control, the same cannot be said for longitudinal dynamics. From now on it will be important, appropriate, and possible, to concentrate more on longitudinal dynamics.

Previous benchmark comparisons of results of ETEAPOT and Runge-Kutta tracking showed seemingly contradictory results. For example ETEAPOT tracking[4] showed long term instability limiting the dynamic aperture to be about an order of magnitude less than given by Runge-Kutta tracking[5]. We have now realized that this inconsistency may be partially understood in terms of the vastly disparate peak RF voltages that were being assumed for the two studies. In both cases harmonic number $h = 100$ was assumed, but the largest peak RF voltage in the ETEAPOT study was 5 KV, whereas, in the Runge-Kutta study the peak voltage was 1 MV. This factor of 200 difference can certainly be expected to affect the comparison. Extending the range of RF voltages in the ETEAPOT study to 0.1 MV (above which instability results) one obtains the comparison shown in Figure 5. This is not intended as evidence of “agreement” between the results; rather it is intended as a beginning on the route to eventual, more controlled, comparison. Complications in performing such comparisons are discussed next.

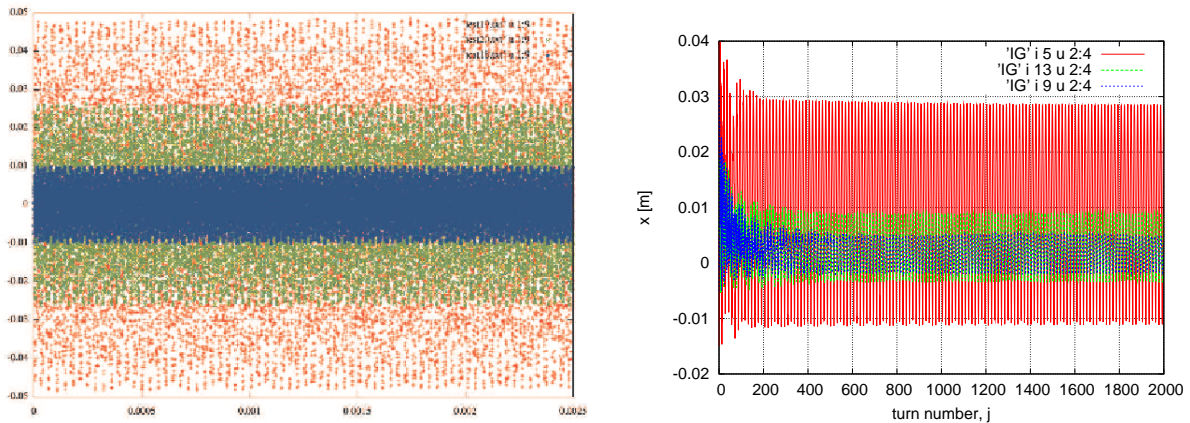


Figure 5: Comparison of (Figure 18 of reference[5]) Runge-Kutta tracking (on the left) with ETEAPOT tracking (on the right). In both cases the three traces correspond to initial x -amplitudes of -1 cm (blue), 0 (green), and +1 cm (red), all with $\Delta p/p = 2 \times 10^{-4}$. The x -ranges of both plots are about the same. For the Runge-Kutta plot the RF voltage was 1 MV. For the ETEAPOT plot the RF voltage was 0.1 MV (approximately the highest voltage for which the particles could be captured into stable buckets). This comparison is discussed (and qualified) further in the text.

Though it has been stated that the same lattice (namely `E_BM_Z-RF.sxf`) has been used in the ETEAPOT/Runge-Kutta comparison, this is only approximately true, especially as regards the (weak) vertical focusing needed to preserve vertical stability. Furthermore the m -values are slightly different. These blemishes are not expected to be significant.

The ETEAPOT/Runge-Kutta comparison in Figure 5 is as close as it is only because various empirical adjustments (for example resolving ambiguous lattice details to make the plots look more similar) have been made. Furthermore, though the three ETEAPOT initial displacements are displaced from each other by 1 cm, they have been allowed to shift together radially to compensate for a possible shift of the fixed point about which linearized expansion is valid. (Allowing this freedom can only be justified as an interim procedure.) Even so, casual observation shows significant disagreements remain, especially the up-down asymmetry on the right but not on the left, and different amplitudes. One hint of difficulty, shared by both plots, is that the +1 cm and -1 cm traces are not the same, except for sign, which is what one might have expected.

While it has been easy to specify transverse-sensitive lattice conditions unambiguously it is harder to specify longitudinal conditions. There is ambiguity as to whether the beam is specified inside or

outside electric field regions; the change in kinetic energy in passing from inside to outside affects this specification. It is also important to specify where in the ring the RF cavity is situated, as beam capture depends on this. If the RF cavity is at the beginning or end of the lattice (as is convenient for such studies) it is essential to know whether the beam is injected just before or just after the RF. More generally, the specification of longitudinal performance depends on the full, six-dimensions in phase space, of the initial bunch distribution.

The fine grain structure of the ETEAPOT and Runge-Kutta plots in Figure 5 are similar. By counting red peaks one finds the “synchrotron tune” Q_s of this granularity to be $Q_s = 14.2/200 = 0.071$ for the ETEAPOT plot. (Though it is not possible to infer it from the fuzzy plot) this is the same for all three traces; see Figure 6. For the outermost (red) Runge-Kutta plot there are 14 periods in 0.0005s, which corresponds to 357 turns. This yields $Q_s = 14/357 = 0.039$. Again, the blue and green peaks are too fuzzy to be counted in the figure as reproduced here. But the plots in the original report[5] are clearer, and there seem to be 15.5 green peaks over the same interval that there are 14 red peaks. If true, it would imply the red and green particles have not been captured in the same bucket. This should be checked.

To illustrate these issues further, Figure 6 shows the longitudinal phase space evolution corresponding to the ETEAPOT data on the right in Figure 5. The most essential aspect of this figure is that the particles are limited to the longitudinal range from -0.8m to +0.8m. In other words, the particles have been captured into a stable bucket. This limitation, specific to capture into a stable bucket, cannot be inferred from Figure 5.

From the comparison of Figures 5 and 6 one sees also that the distribution in transverse amplitude x is strongly correlated with the range in energy spread $\Delta E/p_0 c$. When the three particles were injected (from zero electric potential outside bend elements) their kinetic energies were the same but, inside electric elements, their kinetic energies have become different, both because of the different potentials they had to surmount on entry, and because of the different energies imparted by the RF.

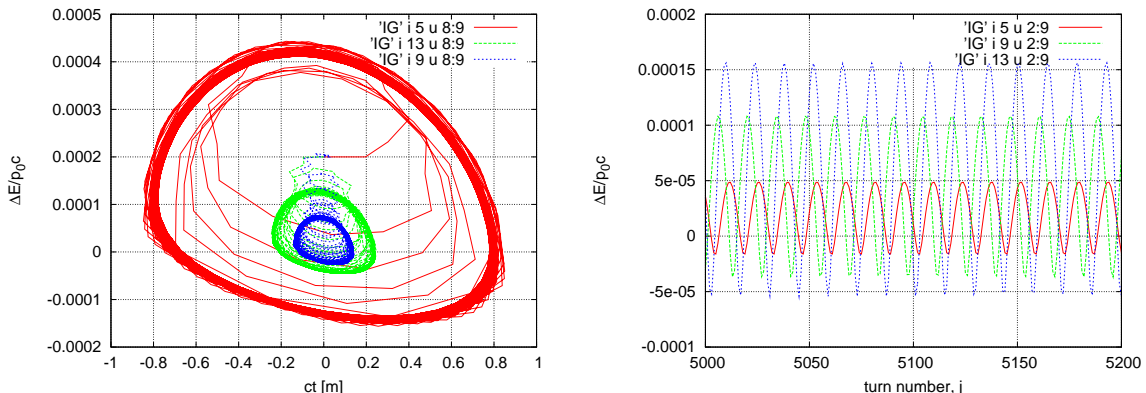


Figure 6: Longitudinal phase space plots corresponding to the ETEAPOT data on the right in Figure 5. The figure on the right checks that the three traces are exactly synchronized, as is required for the particles to be in the same stable bucket.

Comparisons of longitudinal dynamics will eventually require the comparison of entire beam bunches, with realistic spreads in all phase space dimensions. A small step in this direction is indicated in Figure 7.

The figure is based on the longitudinal evolution for 2000 turns of a bunch of 21 particles initially distributed on-momentum, with zero momentum spread, and zero angular spread, but uniformly distributed radially on the range $-5\text{ mm} < x < 5\text{ mm}$. The trace on the left is that of a single particle; its amplitude is more-or-less constant. The trace in the middle is that of the centroid of all 21 particles. Its lack of constancy is due to decoherence, followed by partial recoherence, of the particles of different amplitude. The figure on the right shows the centroid momentum plotted for about ten times as many turns. Though any one particle executes constant betatron plus synchrotron oscillations, the centroid drifts quasi-randomly due to the accidental coherence and decoherence of 21 particles. (With a real beam

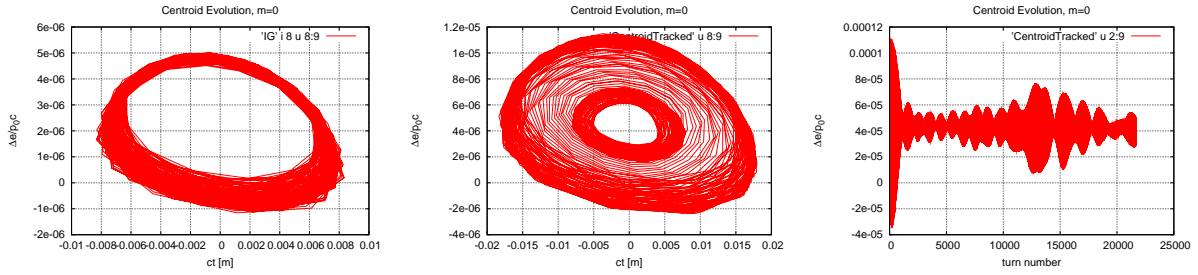


Figure 7: Longitudinal phase space plots, for a single particle on the left, and for the centroid of a bunch of 21 particles in the middle, both for 2000 turns. On the right the transverse momentum is plotted for 21500 turns.

of 10^{10} particles this fluttery variation would be negligible.)

As mentioned in the abstract, attempts to achieve stable capture into the `E_ValLeb2-s14-RF.sxf` lattice have failed so far. This has not been for want of trying. Hundreds of, admittedly disorganized, attempts, including many with the wrong RF frequency, and/or the wrong RF phase, have been made without success so far. In any case this curious result is not understood at present.

References

- [1] V. Lebedev, *Prospects of Strong Horizontal Focusing Electric Ring: Advantages, Disadvantages*, Storage Ring EDM Collaboration Meeting, December 9-10, 2013
- [2] J.D. Talman and R.M. Talman, *UAL/ETEAPOT Results (Augmented) for Proton EDM Benchmark Lattices*, BNL internal report, April 29, 2012
- [3] J.D. Talman and R.M. Talman, *UAL/ETEAPOT Proton EDM Benchmark Comparisons II: Transfer Matrices and Twiss Functions*, BNL internal report, August 30, 2012
- [4] J.D. Talman and R.M. Talman, *UAL/ETEAPOT Proton EDM Benchmark Comparisons III: Dispersion, Longitudinal Dynamics and Synchrotron Oscillations*, BNL internal report, January 10, 2013
- [5] Y.K. Semertzidis et al. *Spin Coherence Time Estimation in an All-Electric Field Using a Precision Tracking Simulation Program (DRAFT)*, BNL internal report, August 28, 2012
- [6] H. Wollnik, *Optics of Charged Particles*, Academic Press, Harcourt Brace Jovanovic, Publishers, 1987
- [7] N. Malitsky, J. Talman, and R. Talman, *Appendix UALcode: Development of the UAL/ETEAPOT Code for the Proton EDM Experiment*, UAL/ETEAPOT documentation (frequently revised), August, 2012
- [8] Storage Ring EDM Collaboration, *A Proposal to Measure the Proton Electric Dipole Moment with 10^{-29} e-cm Sensitivity*, especially Appendix 1. October, 2011